Arthritis Research & Therapy

RESEARCH

Open Access

Atf3 + senescent chondrocytes mediate meniscus degeneration in aging

Jing-Yi Wang[1†], Yao-Hui Liu[1†], Xiao Wang[1], Min Ma[1], Zhang-Yi Pan[1], Ao-Yuan Fan[1], Lai-Ya Lu[1], Zheng Liu[1], Kun Tao[1,3*] and Feng Yin[1,2*]

Abstract

Background Meniscus degeneration contributes to knee arthritis progression, but the cellular and molecular mechanisms of meniscus aging remain poorly understood. We aimed to characterize age-related changes in the rat meniscus using single-cell RNA sequencing (scRNA-seq) and identify key pathogenic cell populations and pathways.

Methods Meniscal tissues from young (12 weeks) and aged (24 months) rats were processed for histology, flow cytometry, and scRNA-seq. Bioinformatics tools, including Seurat, Monocle 2, and CellChat, were used to analyze cellular composition, pseudotime trajectories, and intercellular communication. Senescence-related features and signaling pathways were evaluated.

Results Knee joint of aged rats exhibited higher Osteoarthritis Research Society International (OARSI) scores and synovial inflammation. scRNA-seq revealed three major chondrocyte subpopulations: Sox9 + stable chondrocytes, Fndc1 + fibrochondrocytes, and Atf3 + senescent chondrocytes. Aging caused a significant increase in Atf3 + senescent chondrocytes, characterized by the expression of senescence markers (Cdkn1a/Cdkn2a) and activation of inflammatory pathways such as tumor necrosis factor (TNF) and nuclear factor-κB (NF-κB). These cells were predominantly located at the endpoint of differentiation trajectories. CellChat analysis identified the ANGPTL4-SDC4 axis as a key signaling pathway mediated by Atf3 + cells. Immunostaining confirmed elevated Angiopoietin-Like Protein 4 (ANGPTL4) expression in aged menisci.

Conclusion We identified Atf3 + senescent chondrocytes as a key pathogenic population in the aging meniscus, driving degeneration via the ANGPTL4 pathway. Targeting Atf3 + cells or ANGPTL4 signaling may offer new therapeutic strategies for age-related meniscus degeneration and arthritis.

Keywords Arthritis, Senescence, Meniscus, Chondrocyte, scRNA-seq

† Jing-Yi Wang and Yao-Hui Liu contributed equally to this work.

*Correspondence:
Kun Tao
taokun_714@126.com
Feng Yin
001yinfeng@sina.com
[1]Department of Joint Surgery, Shanghai East Hospital, School of Medicine, Tongji University, Shanghai 200092, China
[2]Shanghai Institute of Stem Cell Research and Clinical Translation, Shanghai 200120, China
[3]Department of Joint Surgery, Ningbo No.6 Hospital, Ningbo, Zhejiang, China

Background

Aging, characterized by the gradual deterioration of physiological functions over time, plays a pivotal role in driving various age-related diseases, including osteoarthritis (OA) [1–4]. Among the multiple risk factors for OA - such as obesity, injury, and genetic predisposition - aging stands out as the most significant driver of disease progression [5–8].

Cellular senescence, a hallmark of aging, is characterized by irreversible cell cycle arrest, mitochondrial dysfunction, and the secretion of pro-inflammatory molecules known as the senescence-associated secretory phenotype (SASP) [9–11]. The SASP comprises diverse cytokines, chemokines, proteases, and growth factors [12], several of which—such as IL-1α, IL-6, p16 (CDKN2A) and monocyte chemoattractant protein 1 (MCP-1)—are abundant in OA joints [13]. Notably, p16 expression is closely correlated with age, and measuring cellular p16 levels has been proposed as a biomarker both for cellular senescence and biological aging [14]. In both murine and human articular chondrocytes, higher p16 expression aligns with reduced production of cartilage-specific extracellular matrix (ECM) proteins (e.g., aggrecan) and elevated expression of ECM-degrading SASP factors (e.g., MMP13, MMP1) [15]. Senescent cells accumulate in joint tissues with age, exacerbating tissue degeneration, perpetuating chronic inflammation, and contributing to the structural and functional decline characteristic of arthritis [6, 7, 16].

The meniscus, a fibrocartilaginous structure essential for joint load distribution, shock absorption, and stability, is highly susceptible to age-related degeneration. Cumulative evidence indicates that meniscal injury, partial or total meniscectomy, and degenerative changes in the meniscus can predispose to—or accelerate—knee OA [17–21]. Aging triggers a series of compositional alterations in the meniscus [22], including changes in collagen, cellular organization, and proteoglycan content, which increase tissue fragility and the risk of degenerative tears [23]. Indeed, these changes elevate the incidence of meniscal tears in older populations, and by altering load distribution onto the tibiofemoral cartilage [24], can further contribute to OA progression. While previous studies have identified meniscus stem/progenitor cells [25–28], suggesting a regenerative potential for repair, research specifically targeting meniscal aging remains relatively sparse.

Recent advances in single-cell RNA sequencing (scRNA-seq) have enabled researchers to dissect the cellular heterogeneity in joint tissues, offering valuable insights into meniscal biology. For instance, Sun et al. [28] identified degenerated meniscus progenitor cells (DegP) in healthy human meniscus and suggested their activation by Interleukin-1β as a potential mechanism of degeneration. Another study by Fu et al. [29] compared cellular compositions in the inner and outer meniscus, revealing microenvironmental differences in healthy and degenerated states. Additionally, Sun et al. [30] explored the cellular landscape of discoid lateral meniscus (DLM), identifying two novel cell clusters, including PreHTC-2, predominantly localized in the white zone of DLM. While these studies provide significant insights into meniscal biology and disease states, they primarily focus on healthy or pathologically degenerated meniscus tissue, leaving a critical gap in understanding how aging reshapes the cellular landscape of the meniscus.

Our findings go beyond traditional models of joint pathology to investigate the impact of aging-associated cellular senescence on the meniscus and its inflammatory microenvironment. Specifically, we hypothesize that aging drives the emergence of distinct pathogenic cell populations and signaling pathways that contribute to meniscus degeneration. Using scRNA-seq and bioinformatics, we aimed to identify key cellular changes in aged menisci and explore potential molecular pathways that may play a role in joint inflammation and degeneration.

Methods

Animal model and histological analysis

Twelve-week-old or 24-month-old SD female rats and C57BL/6 female mice were obtained from Laboratory Animal Research Center, Tongji University. Aged rats with obvious diseases such as tumors or systemic abnormalities were excluded to ensure the validity of experimental results. The rats and mice were anesthetized before euthanasia, and their knee joints were dissected for histological evaluation. Joint tissues were fixed in 4% paraformaldehyde, decalcified in EDTA (0.5 M, pH 8.0). Decalcification was performed for 21 days (3 weeks) for the rat samples and for 7 days (1 week) for the mouse samples, after which the tissues were embedded in paraffin and sectioned (5 μm thick). The sections were then stained with safranin-O or hematoxylin to assess joint morphology and cartilage integrity [31, 32]. Osteoarthritis Research Society International (OARSI) grades and synovitis severity scores were assigned based on previously described scoring systems [33].

For immunohistochemistry, joint sections of mice underwent deparaffinization, rehydration, and antigen retrieval. After blocking (5% BSA), sections were incubated with rabbit anti-ANGPTL4 (1:200; Proteintech, #18374-1-AP) and rabbit anti-ATF3 (1:200; Affinity, #DF3110) at 37 °C for 1 h or 4 °C overnight, followed by HRP-conjugated secondary antibody (1:500) at 37 °C for 30 min. DAB development, hematoxylin counterstaining, dehydration, and mounting were performed for microscopic imaging.

Immunohistochemistry images were captured using the Olympus VS200 slide scanner, while hematoxylin-stained sections were imaged using the Olympus BX63 Microscope.

Micro-CT analysis

Sprague-Dawley (SD) rats were anesthetized with isoflurane and euthanized by cervical dislocation. Knee joints were dissected, fixed in 4% paraformaldehyde for 24 h, and scanned using a NEMO NMC-200 Micro-CT system (Pingsheng Healthcare Technology, <7.5 μm resolution) at 80 kV and 0.06 mA with continuous acquisition (20 frames/sec, 4000 total frames). Scans were performed with 410 mm source-detector distance and 90 mm source-object distance, reconstructed using FDK algorithm (50 mm transverse FOV, 16 mm axial FOV) at $0.05 \times 0.05 \times 0.05$ mm^3 voxel size (35 μm scan precision). Three-dimensional images were acquired using Cruiser and reconstructed with Recon software (v2.0) Quantitative analysis of subchondral bone region focused on trabecular thickness (Tb.Th), bone volume fraction (BV/TV), trabecular separation (Tb.Sp), trabecular number (Tb.N), bone mineral density (BMD) and bone mineral content (BMC) using built-in algorithms.

Tissue dissociation for single-cell RNA-seq

This study included young (12 weeks old, $n = 6$) and aged (24 months old, $n = 5$) Sprague Dawley (SD) rats, corresponding to human early adulthood (20–30 years) and old age (~60 years) [34], respectively. We used 5–6 rats per group to ensure sufficient cell yield for single-cell RNA sequencing, given the limited meniscus tissue size. Meniscal tissues were processed as described previously [28]. Briefly, tissues were minced into ~1 mm^3 pieces, digested with 4 mg/mL protease for 1 h, followed by 0.25 mg/mL collagenase P for 4–6 h. After washing with 0.04% bovine serum albumin (BSA) in phosphate-buffered saline (PBS), the cells were resuspended in 0.04% BSA and filtered through a 35 μm cell strainer. Viable cells were visually inspected, sorted via flow cytometry, and collected. Flow cytometry sorting ensured a viability threshold of >85% for downstream analyses.

Single-cell RNA library Preparation and sequencing

Single-cell RNA-seq libraries were prepared following the Chromium Single Cell 3' Reagent Kit v2 protocol (10×Genomics). Cells were loaded onto a microfluidic chip to generate Gel Beads in Emulsion (GEMs). Within each GEM, mRNA from lysed cells was barcoded, reverse-transcribed into cDNA, and sequenced. Libraries were sequenced on an Illumina HiSeq platform to achieve a depth of ~50,000 reads per cell. Libraries were mapped to the human reference genome (GRCh38-3.0.0) and quantified using Cell Ranger 3.1.0. Raw sequencing data and analysis scripts have been deposited in the Gene Expression Omnibus (GEO) under accession number GSE286034.

Single-cell data processing and analysis

Cell barcode whitelists were identified using UMI-tools. Quality control retained cells expressing over 200 genes and excluded those with >40% mitochondrial UMI counts to remove low-quality cells. Mitochondrial genes were excluded from the expression table. PCA was performed on the top 1000 highly variable genes, and the first 10 principal components were used for t-SNE visualization. Seurat (v4.0.5) was used for clustering, with a resolution parameter of 0.8 to determine cell subpopulations. Cluster marker genes were determined using the Wilcoxon rank-sum test with criteria: lnFC > 0.25, $p < 0.05$, min.pct > 0.1. Cell types were annotated based on canonical markers, and cluster identities were validated with reference datasets.

Pseudo-time analysis and stemness analysis of chondrocyte subpopulations

Pseudo-time trajectory analysis was performed using Monocle 2 [35]. Seurat-processed data were imported into Monocle for trajectory construction. Cells were ordered along a trajectory based on their progression through biological processes such as differentiation. To obtain the degree of differentiation of each subpopulation, R package CytoTRACE v0.3.3 was applied [36]. CytoTRACE scores range from 0 to 1, while higher scores indicate higher stemness (less differentiation) and vice versa.

GO and pathway analysis

Gene ontology (GO) analysis was performed to elucidate the biological significance of differentially expressed genes, using annotations from NCBI (http://www.ncbi.nlm.nih.gov/), UniProt (http://www.uniprot.org/) and Gene Ontology (http://www.geneontology.org/) databases. Fisher's exact test was applied to identify the significant GO categories and FDR was used to correct the p-values. Pathway analysis was conducted with KEGG, identifying significant pathways using Fisher's exact test with thresholds defined by p-value and FDR [37].

Gene set enrichment analysis (GSEA)

Gene expression profiles were analyzed using GSEA to identify enriched pathways. The SenMayo aging gene set database [38] and predefined pro-inflammatory/apoptosis pathways (e.g., TNF signaling, NF-κB activation, SASP regulation) were applied. Normalized expression data were ranked, and enrichment scores were calculated with 1,000 permutations. Significant pathways were defined by false discovery rate (FDR) < 0.25 and nominal $p < 0.05$.

Results highlighted senescence and inflammation-related pathway enrichment in aging chondrocytes.

Senescence score estimation using ssGSEA

Senescence scores were calculated using single-sample gene set enrichment analysis (ssGSEA [39]) with the SASP and SenMayo [38] gene sets via the GSVA R package. Enrichment scores, derived from gene expression ranks, quantified senescence activity. Scores were normalized across samples and assessed for statistical significance to evaluate senescence levels.

Quantitative real-time PCR (RT-qPCR)

Total RNA was extracted using the RNeasy Plus Mini Kit (Qiagen) following the manufacturer's instructions. RNA was eluted with 30 μL RNase-Free H_2O, quantified using a Nanodrop, and reverse transcribed with ABScript Neo RT Master Mix (ABclonal). RT-qPCR was performed using 2× ChamQ Blue SYBR qPCR Master Mix (Vazyme) on a QuantStudio 6 Flex, with reactions in duplicates or triplicates. Relative expression levels were calculated using the $2-\Delta CT$ or $2-\Delta\Delta CT$ method, with GAPDH as the reference gene. The primers used for target gene amplification were: Angptl4 (F: 5′-CGCTTACACAGGC CTCCC-3′, R: 5′-ATGGTGGAGATCCCAGAGGC-3′), Atf3 (F: 5′-GACAGCCCGCCTCTAGC-3′, R: 5′-GAAG CATCATTTTGCTCCAGTC-3′), Cdkn1a (F: 5′-TTGTG ATATGTACCAGGACTGC-3′, R: 5′-CCCTCTCCCCCA GTAAGTTTC-3′).

Ethics statement

All animal procedures complied with the Guidelines for the Care and Use of Laboratory Animals of the National Institutes of Health and were approved by the Animal Care and Use Committee of Tongji University (approval code: TJBB03921401). Experiments were conducted following ARRIVE guidelines, and efforts were made to minimize animal suffering.

Statistical analysis

Statistical analyses were performed using Prism 10.0. Normality was tested via Shapiro-Wilk ($p > 0.05$). Normally distributed data were compared with unpaired *t*-tests (two groups) or one-way ANOVA (≥ 3 groups) with Tukey's post hoc test. For non-parametric datasets, the Kruskal-Wallis H test with Dunn's post hoc test was applied. Results are expressed as mean ± SD (parametric) or median with range (non-parametric). A p-value < 0.05 was considered statistically significant.

Results

Single-cell transcriptomic reveals the cellular landscape of young and aged meniscus

To investigate the histological and cellular changes in aging knee joints, we performed a comprehensive histological assessment in both aging mice and rats. Safranin O/Fast Green staining of articular cartilage revealed chondrocyte degeneration in aged rats joints compared to young controls, with higher Osteoarthritis Research Society International (OARSI) scores (Fig. 1A, C). Hematoxylin and Eosin (H&E) staining further indicated synovial hyperplasia in aged rats. Elevated synovial scores highlight the role of synovial inflammation in joint aging (Fig. 1B, C). Safranin O/Fast Green staining in mice showed similar findings (Fig. S1A, B). Additionally, micro-CT analysis of the tibial subchondral bone in aged rats revealed typical structural alterations (Fig. 1D; Fig. S1C). Trabecular thickness (Tb.Th) showed a marked increase, accompanied by elevated bone volume fraction (BV/TV) (Fig. 1E), indicating enhanced bone remodeling. Concurrently, decreased trabecular number (Tb.N) and increased trabecular separation (Tb.Sp) (Fig. S1D) were observed, reflecting compromised trabecular connectivity in aged rats. Also, while bone mineral density in the aged group exhibited an upward trend compared to the young group, this difference did not reach statistical significance (Fig. S1D). In contrast, bone mineral content was significantly elevated in the AM group (Fig. S1D), suggesting increased mineral accumulation despite unaltered density. These changes collectively pointed to subchondral bone sclerosis with distinct microarchitectural and compositional dysregulation.

To uncover the cellular composition and molecular profiles of meniscal cells from different age groups, we conducted single-cell RNA sequencing (scRNA-seq) analysis using the 10x Chromium platform (Fig. 2A). Meniscus tissue was enzymatically digested into single-cell suspensions, and flow cytometry was employed to isolate viable cells. Preliminary flow cytometry analyses also identified CD45 + cells, representing hematopoietic cells originating from the ossified marrow cavity. (Fig. S1D). We used the Seurat pipeline for unbiased clustering, yielding 11 distinct clusters from young (YM) and aged (AM) meniscus. Uniform manifold approximation and projection (UMAP) visualization showed clear segregation of cell populations (Fig. 2B), with cluster identities determined based on the expression of canonical marker genes (Fig. 2D, Fig. S2A-J). For instance, chondrocytes were identified by high expression of cartilage-related genes as previously described [29], including Dcn, Sparc, Gsn, Comp, Col1a1 and Col3a1 (Fig. 2D). Sample origin mapping confirmed minimal batch effects and preserved biological variations between YM and AM groups, ensuring reliable downstream analyses (Fig. 2C).

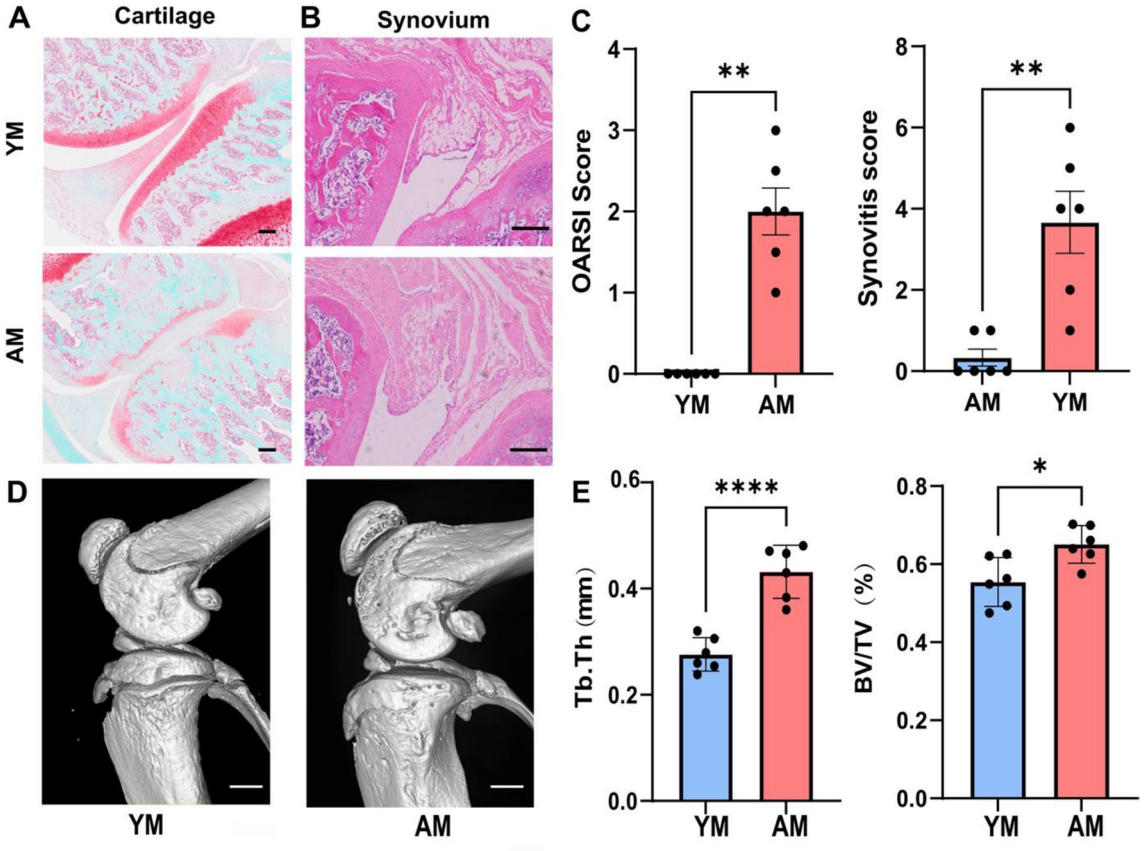

Fig. 1 Histological analysis reveals age-related changes in mice meniscus (**A**) Safranin O/Fast Green staining of articular cartilage in young and aged rats. Scoring was performed independently by two experienced pathologists in a blinded manner to ensure objective evaluation. Scale bar: 100 μm (**B**) Representative hematoxylin and eosin (H&E) staining of synovial tissue in young and aged rats, showing age-associated synovial inflammation. Scale bar: 100 μm. (**C**) Quantification of the OARSI score and synovitis score in young and aged rats. (**D**, **E**) Micro-CT evaluation of the tibial subchondral bone revealed significant age-related changes. (**D**) Representative 3D reconstructed images of the tibial subchondral bone from young (YM) and aged (AM) rats. (**E)** Quantitative analysis of trabecular thickness (Tb.Th) and bone volume fraction (BV/TV) in the young and aged group. Scale bars: 5 mm.Statistical significance was assessed using one-way ANOVA followed by Tukey's multiple comparison test (*$p < 0.05$, **$p < 0.01$, ***$p < 0.001$)

Differential gene expression analysis between YM and AM groups revealed significant age-related transcriptional changes. Gene Ontology (GO) enrichment analysis highlighted upregulated pathways in AM, such as cellular response to interferon-gamma, cellular response to interleukin-1, and apoptotic process (Fig. 2E). Consistently, qPCR validation demonstrated increased expression of the senescence marker Cdkn1a (p21) in aged menisci (Fig. S2L), further corroborating the tissue's aged phenotype. Downregulated pathways were associated with core cellular functions, including transcriptional regulation, RNA processing, and chromatin remodeling, suggesting age-related functional decline (Fig. 2F). Gene Set Enrichment Analysis (GSEA) also confirmed significant enrichment of the TNF signaling pathway in aged cells (Fig. S2K). Together, these results indicate that the aged meniscus exhibits progressive loss of tissue integrity and a shift toward a pro-inflammatory phenotype.

Identification of three chondrocyte subpopulations

To investigate changes in chondrocytes during aging, we observed 261 upregulated genes and 544 downregulated genes in aged rats chondrocytes compared to the young group (Supplement Table 1). Gene Ontology (GO) biological process (BP) enrichment analysis demonstrated significant downregulation of extracellular matrix (ECM) organization, collagen fibril organization, and other cartilage-related pathways in AM chondrocytes., reflecting their role in maintaining tissue integrity and indicating dysfunction during aging (Fig. S3A). We identified a set of stage-specific signature genes with potential to promote aging, such as Gpx3, Ifi27l2b, and Cxcl1, whereas another set of signature genes exhibited potential protective characteristics, including Sparc and Snorc (Fig. 3A). Gene Set Enrichment Analysis (GSEA) further supported the presence of pro-inflammatory and apoptosis pathways, including TNF signaling, NF-κB activation, and SASP regulation (Fig. 3D). Notably, we utilized SenMayo [38], an aging gene set database developed by Dominik

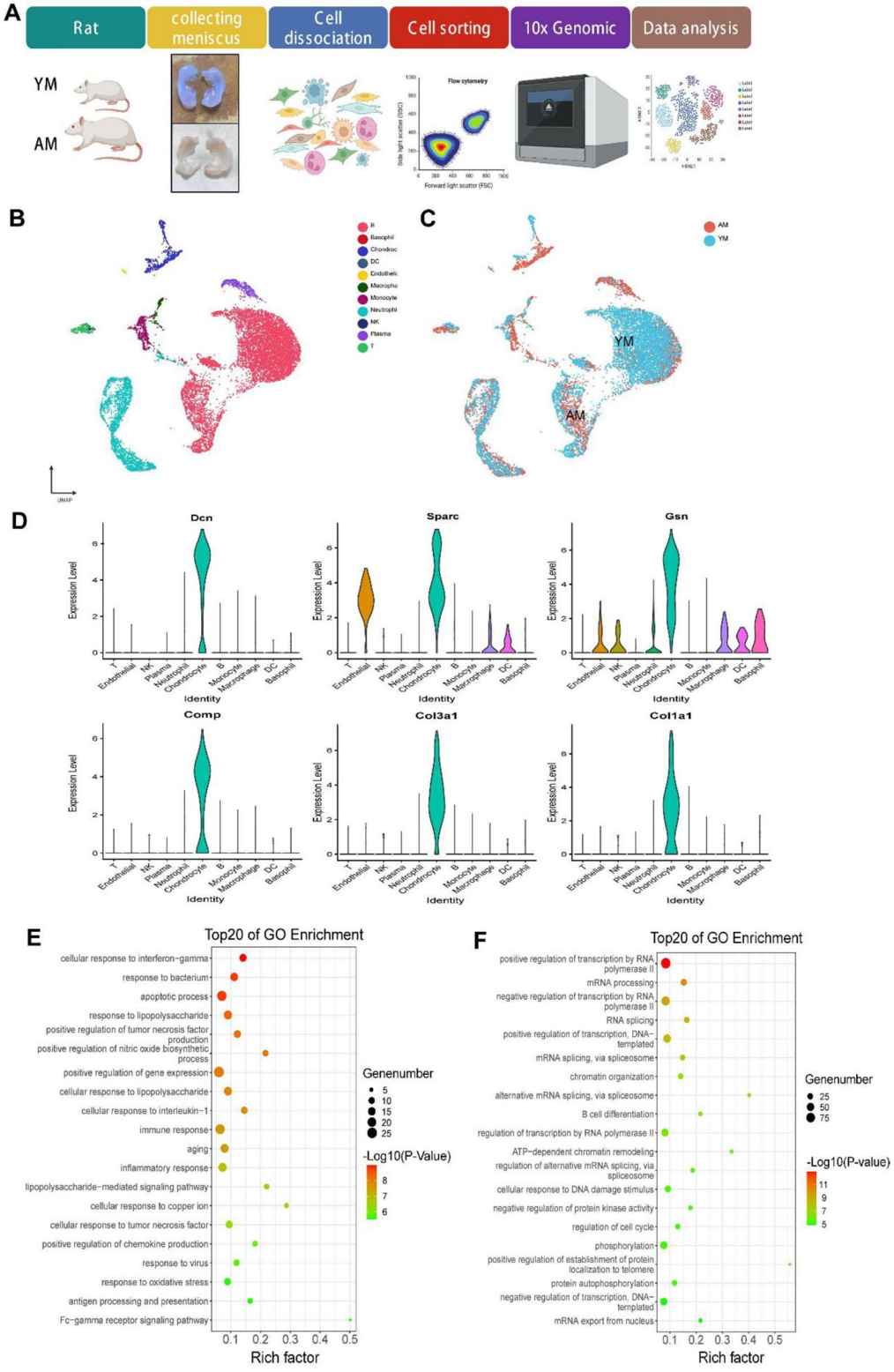

Fig. 2 Single-cell transcriptomic profiling of meniscal cells in young and aged rats. (**A**) Workflow of single-cell RNA sequencing (scRNA-seq) applied to meniscal tissue. (**B**) UMAP visualization showing 11 cell clusters identified in young (YM) and aged (AM) meniscal samples. (**C**) Sample origin mapping reveals minimal batch effects across YM and AM groups. **(D)** Violin plots of canonical marker genes indicating chondrocytes. (**E**, **F**) Gene Ontology (GO) enrichment analysis for differentially expressed genes between YM and AM. (**E**) GO terms enriched in genes upregulated in AM. (**F**) GO terms enriched in genes downregulated in AM. X-axis: Rich factor; Y-axis:–log10(p-value)

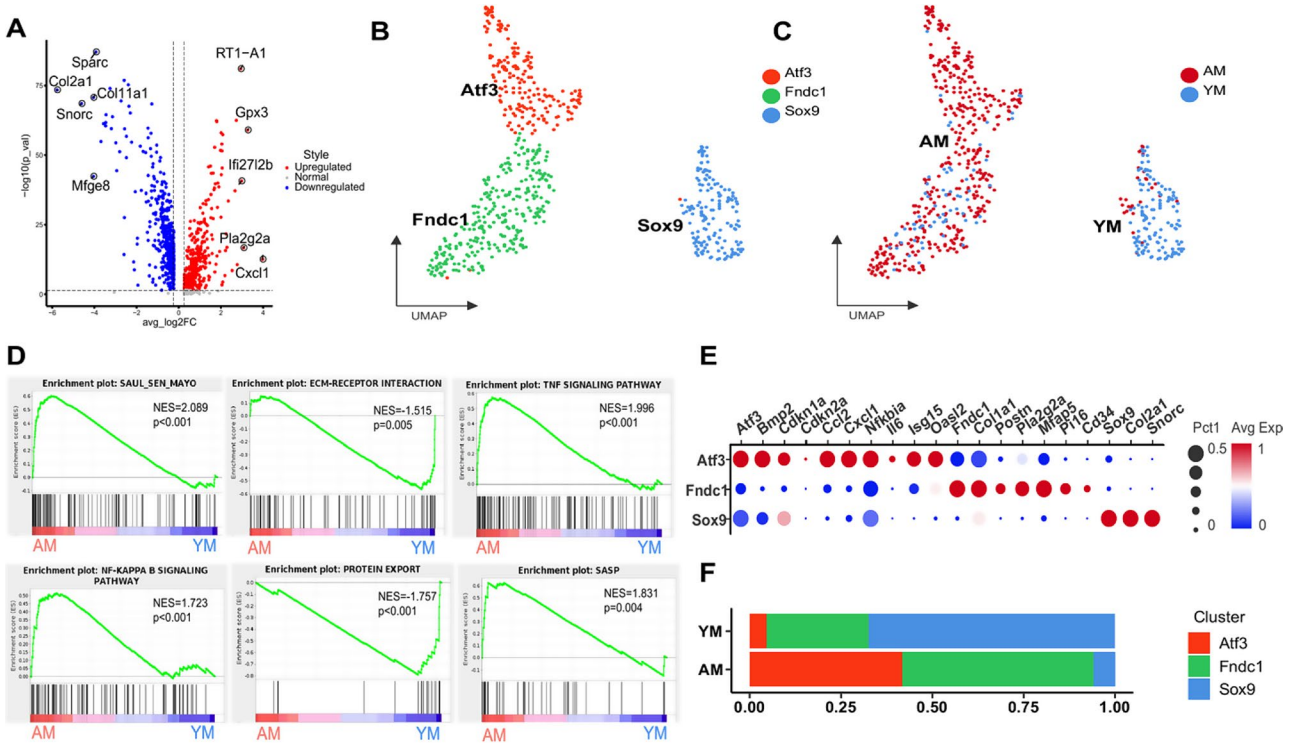

Fig. 3 Transcriptional heterogeneity of chondrocytes in the meniscus of young and aged rats. (**A**) Volcano plot showing differentially expressed genes between young and aged chondrocytes. (**B**) UMAP visualization identifying three chondrocyte clusters. (**C**) UMAP visualization identifying two samples. (**D**) Gene Set Enrichment Analysis (GSEA) indicating several highly enriched pathways in aged chondrocytes. (**E**) GeneExpBubblePlot showing normalized expression of differentially expressed genes in each chondrocyte cluster. (**F**) Proportion of each chondrocyte cluster in the meniscus of young and aged rats

Saul and colleagues, which demonstrated that senescence-related pathways were highly enriched in chondrocytes from the aging group. These findings highlight the dual roles of aging-associated factors in promoting degeneration while disrupting homeostasis.

To gain a deeper understanding of the changes in chondrocytes during aging, we performed refined re-clustering. Visualized through UMAP, chondrocytes were categorized into three distinct subclusters based on gene profiles and canonical markers (Fig. 3B, C). Specifically, these subclusters included: proliferative fibrochondrocytes (Sox9+), senescent chondrocytes (Atf3+), and fibrochondrocytes (Fndc1+). The Sox9 + subcluster highly expressed Col2a1 and Snorc; the Atf3 + subcluster expressed Ccl2, and Bmp2; and the Fndc1 + subcluster expressed Col1a1, Postn, and Pla2g2a (Fig. 3E). Significantly, scRNA-seq analysis uncovered variations in cell type composition between young and aged meniscus, indicating a high heterogeneity among meniscus chondrocytes. We observed a significant decrease in the proportion of Sox9 + homeostatic chondrocytes from 67.4% in young rats to 5.9% in aged rats, while Atf3 + senescent chondrocytes increased significantly from 4.7% in young rats to 41.9% in aged rats (Fig. 3F). This transition suggests a marked loss of chondrocyte homeostasis and a concomitant escalation in senescence with aging. In addition to the substantial increase in Atf3 + chondrocytes in the aged group, we also found that Cdkn1a and Cdkn2a (Fig. 3E) were highly expressed in Atf3 + chondrocytes, leading us to propose that this cell group may represent an age-related pathogenic cluster.

Atf3+ subset is a senescent chondrocyte population in aged meniscus

To understand the biological processes dysregulated in this pathogenic cluster, we performed gene ontology (GO) analysis. Genes highly expressed in Atf3 + cells were predominantly associated with aging, inflammatory response, and hypoxia, reflecting a stress-related phenotype (Fig. 4A). Pathway enrichment analysis further identified multiple significantly upregulated pathways in the Atf3 + cluster, culminating in pivotal signaling pathways such as p53, MAPK, NF-κB, apoptosis, and TNF signaling (Fig. 4B, C; Fig. S3B). The SCENIC analysis of Atf3 + chondrocytes identified key transcription factors driving their pro-inflammatory and pathogenic profile. NFKB1 and NFKB2, central regulators of inflammatory signaling, were significantly activated, aligning with the enrichment of pathways associated with inflammation, extracellular matrix turnover, and oxidative

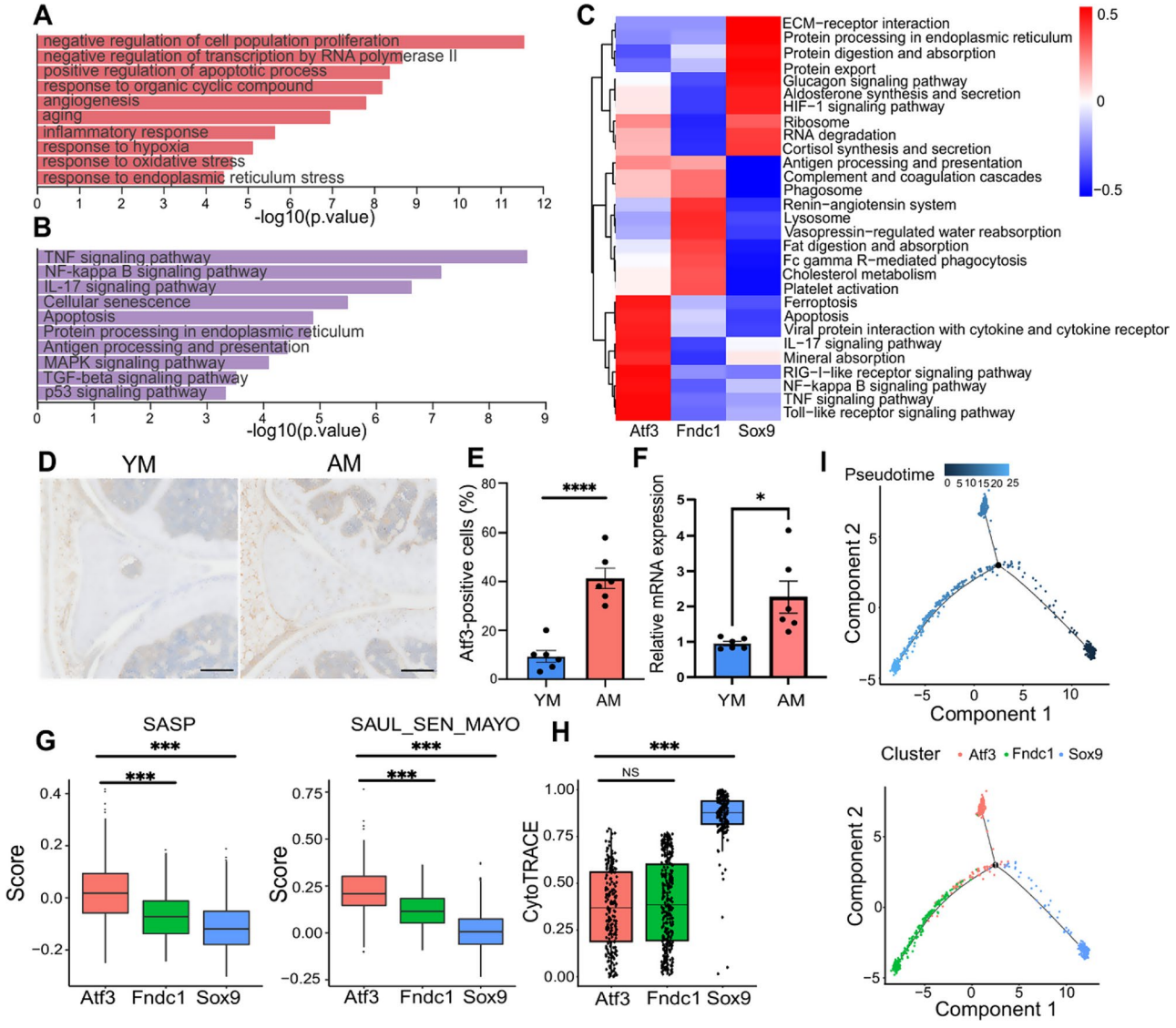

Fig. 4 The Atf3 + subset identified as a senescent chondrocyte population. (**A**, **B**) Gene Ontology(A) enrichment and KEGG analysis(**B**) for differentially expressed genes in Atf3 + chondrocytes of meniscus. X-axis:–log10(p-value);p < 0.001 (**C**) Heatmap showing the enrichment of key biological pathways in chondrocyte subpopulations. (**D**, **E**) Representative immunohistochemistry (IHC) staining of Atf3 in young and aged mouse menisci, and quantification of Atf3-positive cells. Scale bar: 100 μm. Con, n = 6; Aged, *n* = 6. ****$p < 0.0001$. (**F**) The relative expression levels of Atf3 were quantified by qPCR, demonstrating differential expression between young and aged mice. Con, *n* = 6; Aged, *n* = 6. *p < 0.05 (**G**) Boxplot of single-sample Gene Set Enrichment Analysis (ssGSEA) of each chondrocyte subset. ***$p < 0.001$ (**H**) CytoTRACE analysis of the three subsets.***p < 0.001 (**I**) Pseudotime progression diagram, with color from dark to light indicating the pseudo-time order (top). The pseudo-temporal map of chondrocytes is colored according to cell subtype (bottom)

stress, emphasizing the contribution of Atf3 + chondrocytes to joint degeneration and OA progression (Fig. S3C). Meniscal tissue from aged mice showed a marked increase in Atf3 + chondrocytes compared to their young counterparts (Fig. 4D, E), which was corroborated by qPCR analysis showing elevated Atf3 mRNA expression in aged menisci (Fig. 4F), collectively confirming the transcriptional and cellular accumulation of Atf3 during aging. To substantiate these observations, we further used Single-Sample Gene Set Enrichment Analysis (ssGSEA) to assign SASP and SenMayo senescence scores to each chondrocyte cluster. The Atf3 + subset exhibited the highest SASP and SenMayo scores, further supporting its pathogenic role in the aging meniscus (Fig. 4G).

To infer the differentiation trajectories of chondrocytes, we performed pseudotime analysis. Chondrocytes from the young group were predominantly distributed at the beginning of the pseudotime trajectory, while aging group chondrocytes were concentrated at the trajectory's endpoint (Fig. S3D). Within specific subgroups, Sox9 + stable chondrocytes occupied the initial pseudotime positions, while Atf3 + senescent chondrocytes were located at the terminal end (Fig. 4I). Although the CytoTRACE scores for Atf3 + cells were numerically lower

than those for Fndc1 + cells (indicating potentially lower differentiation potential), the difference did not reach statistical significance ($p = 0.14$) (Fig. 4H). However, considering the highest SASP and SenMayo scores (Fig. 4F) observed in Atf3 + cells, these integrated findings suggest that the Atf3 + subset represent a senescent, highly pathogenic population contributing to meniscal degeneration.

Alterations in individual signaling pathways in the aging and young chondrocyte groups

To elucidate the interplay among the three distinct chondrocyte subpopulations, we employed CellChat analysis, comparing interaction intensities between young and aged samples based on ligand-receptor expression. By comparing global signaling intensities between young and aged groups, we identified conserved and aging-specific pathways (Fig. 5A, B). Pathways highlighted in red were enriched in the aged group, while green-highlighted pathways were more active in the young group. Among these pathways, the ANGPTL pathway emerged as remarkably enriched in the aged group. Comparative analysis of the overall signaling patterns among the three chondrocyte subpopulations revealed that the ANGPTL pathway played a pivotal role in both outgoing and incoming signaling contributions within the Atf3 + subpopulation (Fig. 5C). Specifically, in the aged group, the most prominent receptor-ligand pair driving the ANGPTL pathway was Angptl4-Sdc4 (Fig. 5D). ANGPTL4 [40], an angiopoietin-like protein induced by hypoxia, has been reported to accumulate in the ECM remodeling and degradation in arthritic cartilage. Consistently, Atf3 + chondrocytes exhibited significantly elevated ANGPTL4 expression (Fig. 5E), with concomitant upregulation of Angptl4 mRNA levels in aged menisci demonstrated by qPCR (Fig. 5H), further validated by IHC staining (Fig. 5F, G). These results underscore the critical role of the ANGPTL pathway, mediated by Atf3 + chondrocytes, in the pathological progression of meniscal aging.

Discussion

In this study, we conducted a comprehensive examination of aging rat joint tissues, providing critical insights into the intricate cellular and molecular dynamics underlying age-related joint degeneration. Distinct pathological features, including chondrocyte degeneration and synovial hyperplasia, were observed in aged joint tissues, consistent with OA-related changes. These findings align with previous studies highlighting the interplay between meniscal degeneration and synovial inflammation in OA [41, 42]. Micro-CT quantification further revealed a paradoxical subchondral bone remodeling pattern in aged (AM) group, characterized by elevated bone volume fraction (BV/TV), trabecular thickness (Tb.Th) and bone mineral content (BMC), concomitant with decreased trabecular number (Tb.N) and increased trabecular separation (Tb.Sp). This 'high-mass, low-quality' microarchitecture conforms to the hallmark of subchondral sclerosis [43], where compensatory bone formation thickens trabeculae at the expense of structural homogeneity, ultimately compromising biomechanical competence.

Signature gene analysis identified aging-associated molecular changes, including the enrichment of pro-aging genes (e.g., Gpx3, Ifi27l2b, and Cxcl1) and the downregulation of protective genes like Sparc and Snorc in aged cartilage tissues. Sparc plays a key role in ECM organization [44], contributing to cartilage integrity, while Snorc [45], a cartilage-specific proteoglycan, is essential for chondrocyte function. Their reduced expression in aging underscores potential therapeutic targets to counteract degeneration.

Subsequent single-cell analysis of meniscal tissues further identified three distinct chondrocyte subpopulations: proliferative fibrochondrocytes (Sox9+), fibrochondrocytes (Fndc1+) and senescent chondrocytes (Atf3+). Notably, aged menisci showed a marked decrease in Sox9 + homeostatic chondrocytes and an accumulation of Atf3 + senescent chondrocytes. The Atf3 + chondrocyte subset exhibited a unique senescence-associated phenotype, with upregulation of senescence markers (e.g., Cdkn1a, Cdkn2a) and pro-inflammatory SASP components (e.g., Cxcl1, Ccl2), indicative of a senescence-associated, growth-arrested phenotype. Consistent with these findings, pseudotime trajectory analysis positioned Atf3 + chondrocytes at the terminal end of differentiation, suggesting an irreversible loss of regenerative capacity. By contrast, Fndc1 + fibrochondrocytes exhibited progenitor-like characteristics and show high expression of Pi16, Mfap5, and Cd34, Consistent with previous single-cell fibroblast studies [46, 47]. Although the CytoTRACE score difference between Atf3 + and Fndc1 + cells was statistically nonsignificant ($p = 0.14$), the lower differentiation potential trend in *Atf3* + cells aligns with their elevated senescence markers (e.g., SASP genes). Technical constraints in trajectory inference or compensatory senescence mechanisms may underlie this discrepancy, warranting functional validation in expanded cohorts.

ATF3 belongs to the ATF/cyclic AMP response element-binding (CREB) protein family of transcription factors. The pathogenic role of Atf3 + chondrocytes aligns with prior evidence that ATF3 deficiency alleviates OA progression [48] and suppresses cyclin D1/A transcription, thereby modulating cell cycle arrest [49]. Recent bioinformatics analysis further suggests that ATF3 may serve as a diagnostic marker for early OA, with dysregulation linked to ferroptosis-related RNA metabolic dysfunction [50]. Furthermore, Single-cell transcriptomic analysis reveals that ATF3 regulates calcification

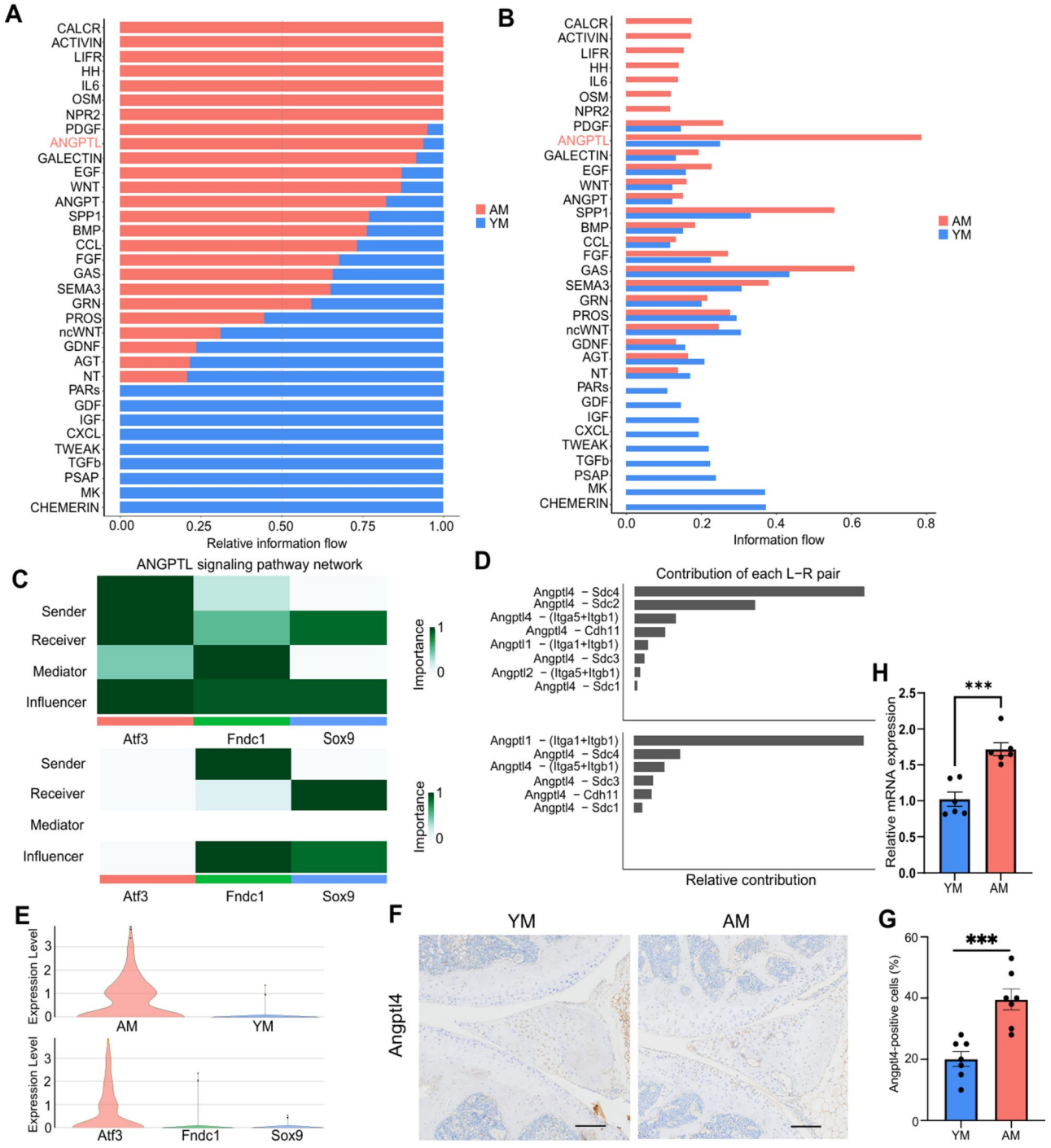

Fig. 5 Alterations in individual signaling pathways in aging and young chondrocyte groups. (**A**) Information flow among young and aged meniscus chondrocytes. Pathways in red are enriched in the aging meniscus chondrocytes, while those in green are enriched in the young meniscus chondrocytes. (**B**) Bar chart displaying differences in the relative ratio of information flow in the interaction network between the aging and young meniscus chondrocytes. (**C**) Degree and differences of the ANGPTL signaling pathway network in chondrocytes from the young (top) and aged (bottom) meniscus. (**D**) The most prominent receptor-ligand pair contributing to the ANGPTL pathway in young and aged groups. (**E**) Violin plots showing the expression of Angptl4 in aged vs. young groups (top) and among three chondrocyte subsets (bottom). (**F**, **G**) Representative immunohistochemistry (IHC) staining of Angptl4 in young and aged mice meniscus, and quantification of Angptl4-positive cells. Scale bar: 100 μm. Con, $n=6$; Aged, $n=6$. $^{****}p<0.0001$. (**H**) The relative expression levels of Angptl4 were quantified by qPCR, demonstrating differential expression between young and aged mice. Con, $n=6$; Aged, $n=6$. $^{***}p<0.001$

in CRTAC1 + chondrocyte-like cells and interacts with SPP1 + macrophages, contributing to ligament degeneration and osteophyte formation [51]. These findings suggest that ATF3 may actively drive joint degeneration, further supported by its role in promoting senescence-like phenotypes.

Our findings regarding Atf3 + senescent chondrocytes resonate with the work of Sun et al. [28], which identified a BMP2 + FOSL1 + regulatory chondrocyte (RegC) cluster in human meniscus. RegC, similar to the Atf3 + subgroup, was predominantly distributed at the terminal points of pseudotime trajectories, suggesting a shared role in late-stage differentiation or stress response. However, Sun et al. did not explore the specific involvement of RegC in aging. This raises the intriguing possibility of a conserved regulatory mechanism involving senescent chondrocytes across species. Future studies should aim to validate this hypothesis in human tissues and explore the specific molecular mechanisms underlying this conserved phenotype. Recent findings also point to specific molecular markers implicated in aging menisci. For instance, the diagnostic marker lactotransferrin (LTF) [52], overexpressed in aged menisci, promotes senescence and degenerative changes via NF-κB pathway. Likewise, a transcriptome-based study identified four key hub genes (RRM2, AURKB, CDK1, TIMP1) and several regulating miRNAs [53] as possible biomarkers for aging-related meniscal tears. It is worth noting that recent studies suggest senescent cells are not invariably detrimental in every context. For example, while eliminating senescent cells using ABT-263 (a pro-apoptotic drug targeting senescent cells) proves beneficial in a rat OA model [54], removing senescent cells during meniscus repair in another rat model instead leads to impaired meniscal regeneration [55]. This finding highlights the stage- and context-dependent nature of senescent cells in joint diseases.

Through intercellular communication analysis, we observed a notable upregulation of the ANGPTL4-SDC4 axis in aged menisci, primarily driven by Atf3^{+} senescent chondrocytes. Angiopoietin-like protein 4 (ANGPTL4), a member of the ANGPTL family, plays a crucial role in regulating lipid metabolism [56–59]. Upon secretion, ANGPTL4 is cleaved into N- and C-terminal (cANGPTL4)—each of which has been implicated in various pathological processes [60].

Growing evidence suggests ANGPTL4 promotes osteolytic erosion, angiogenesis, and increased vascular permeability in arthritic tissues [60–63]. Its overexpression in chondrocytes and synovial cells appears to disrupt joint homeostasis. In RA models, for instance, inhibiting ANGPTL4 reduces fibroblast-like synoviocyte (FLS) invasion and migration, thereby restricting osteoclast activation [64]. Microarray studies [65–67] have further demonstrated ANGPTL4 overexpression in cartilage obtained from non-traumatic osteonecrosis of the femoral head, OA [65], and porcine osteochondrosis [66], as compared with control cartilage. Similarly, in anteromedial knee OA [67], higher ANGPTL4 levels have been noted in damaged cartilage relative to undamaged. During MSC-based chondrogenesis, ANGPTL4 fosters ECM degradation, reduces aggrecan and collagen deposition, and enhances MMP1/MMP13 release. Conversely, silencing ANGPTL4 suppresses SIRTUIN 1/NF-κB–mediated inflammation in chondrocytes, thereby attenuating OA in a DMM mouse model [68].

cANGPTL4 inhibition has emerged as a promising therapeutic avenue. Neutralizing cANGPTL4 protects lung tissue from inflammation-induced damage [69] and inhibits FLS-mediated invasion and osteoclast activation, also pointing to a role in mitigating joint destruction [64].

Moreover, recent scRNA-seq analyses reveal that ANGPTL4 is predominantly localized to subchondral lineages [70], including adipocytes and bone vasculature, underscoring its involvement in subchondral bone remodeling and vascular homeostasis. Other research links ANGPTL4 to lipid accumulation or senescence [71] in renal tubular epithelial cells and cardiomyocyte senescence [72] in diabetic cardiomyopathy (DCM). These findings underscore ANGPTL4's extensive regulatory role in age-associated tissue degeneration and inflammatory processes beyond the joint environment. Our findings extend these observations by establishing, for the first time, ANGPTL4's contribution to age-related meniscus degeneration. Consequently, targeting ANGPTL4 presents a promising strategy for alleviating inflammation and slowing OA progression in aging joints.

Additionally, the substantial presence of B cells in aged meniscal tissues highlights the significance of immune-chondrocyte interactions in joint aging. Although our study did not focus on immune cells, growing evidence suggests their pivotal role in mediating inflammatory responses and disrupting joint homeostasis [73].

Despite these robust findings, certain limitations of this study should be noted. Our use of aged rat models may not fully capture the complexity of human joint aging, and fewer chondrocyte subpopulations were identified compared to studies on human menisci. We acknowledge that selecting five-six rats per group was mainly to ensure sufficient cell yield for single-cell RNA sequencing rather than based on a formal sample size calculation. Although practical given tissue size, cost, and ethical constraints, this approach might limit the detection of subtle transcriptional differences. Future studies with larger sample sizes may help validate and extend these findings. Also, future studies should include scRNA-seq data from human menisci across various age groups to validate these results. Additionally, while this study focused on

meniscal tissues, integrating analyses of other joint components, such as articular cartilage and synovium, could provide a more holistic view of age-related joint changes. Finally, it remains to be tested whether ANGPTL4 inhibition could directly protect the entire joint microenvironment and delay joint aging, which will be an important direction for future translational research.

Conclusions

In summary, this study highlights significant cellular and molecular alterations within aging meniscal tissues, emphasizing the role of Atf3 + senescent chondrocytes and the ANGPTL4 pathways in age-related joint degeneration. These findings establish a foundation for future investigations into therapeutic approaches aimed at preserving joint health in aging populations, with particular focus on the ANGPTL4 pathway.

Abbreviations

scRNA-seq	Single-cell RNA sequencing
OA	Osteoarthritis
RA	Rheumatoid arthritis
YM	Young meniscus
AM	Aged meniscus
OARSI	Osteoarthritis Research Society International
GEO	Gene Expression Omnibus
RegC	Regulatory chondrocyte
ssGSEA	Single-Sample Gene Set Enrichment Analysis
GO	Gene ontology
SASP	Senescence-associated secretory phenotype
H&E	Hematoxylin and Eosin

Supplementary Information

The online version contains supplementary material available at https://doi.org/10.1186/s13075-025-03566-z.

Supplementary Material 1

Supplementary Material 2

Acknowledgements

Not applicable.

Author contributions

JW and YL designed the study and conducted the primary experiments. Both authors contributed equally and are recognized as co-first authors. XW contributed significantly by performing several additional experiments during the revision process. MM, AF and LL were responsible for single-cell sequencing preparation and processing. ZP and ZL handled animal tissue sectioning. KT and FY drafted the manuscript, contributed equally, and share corresponding authorship. All authors reviewed the manuscript.

Funding

This work was sponsored by Cell and Gene Therapy Project of Science and Technology Committee of Shanghai (23J11900400), Peak Disciplines (Type IV) of Institutions of Higher Learning in Shanghai, The Ministry of Science and Technology of China (2020YFC2002800). Abstract figure and Partial elements of Fig. 2A were created in BioRender. Ospelt, C. (2025) https://BioRender.com/b78j667.

Data availability

Raw sequencing data and analysis scripts have been deposited in the Gene Expression Omnibus (GEO) under accession number GSE286034.

Declarations

Ethics approval and consent to participate

Not applicable.

Consent for publication

Not applicable.

Competing interests

The authors declare no competing interests.

Received: 4 February 2025 / Accepted: 2 May 2025
Published online: 15 May 2025

References

1. López-Otín C, Blasco MA, Partridge L, et al. Hallmarks of aging: an expanding universe. Cell. 2023;186:243–78.
2. Martel-Pelletier J, Barr AJ, Cicuttini FM, et al. Osteoarthritis. Nat Rev Dis Primer. 2016;2:16072.
3. McCulloch K, Litherland GJ, Rai TS. Cellular senescence in osteoarthritis pathology. Aging Cell. 2017;16:210–8.
4. Jeon OH, David N, Campisi J, et al. Senescent cells and osteoarthritis: a painful connection. J Clin Invest. 2018;128:1229–37.
5. Johnson VL, Hunter DJ. The epidemiology of osteoarthritis. Best Pract Res Clin Rheumatol. 2014;28:5–15.
6. Coryell PR, Diekman BO, Loeser RF. Mechanisms and therapeutic implications of cellular senescence in osteoarthritis. Nat Rev Rheumatol. 2021;17:47.
7. Loeser RF, Collins JA, Diekman BO. Ageing and the pathogenesis of osteoarthritis. Nat Rev Rheumatol. 2016;12:412.
8. Rahmati M, Nalesso G, Mobasheri A, et al. Aging and osteoarthritis: central role of the extracellular matrix. Ageing Res Rev. 2017;40:20–30.
9. Campisi J. Aging, cellular senescence, and cancer. Annu Rev Physiol. 2013;75:685–705.
10. Wolfenson H, Yang B, Sheetz MP. Steps in mechanotransduction pathways that control cell morphology. Annu Rev Physiol. 2019;81:585.
11. Victorelli S, Salmonowicz H, Chapman J, et al. Apoptotic stress causes MtDNA release during senescence and drives the SASP. Nature. 2023;622:627–36.
12. Freund A, Orjalo AV, Desprez P-Y, et al. Inflammatory networks during cellular senescence: causes and consequences. Trends Mol Med. 2010;16:238–46.
13. Tsuchida AI, Beekhuizen M, 't Hart MC, et al. Cytokine profiles in the joint depend on pathology, but are different between synovial fluid, cartilage tissue and cultured chondrocytes. Arthritis Res Ther. 2014;16:441.
14. Krishnamurthy J, Torrice C, Ramsey MR, et al. Ink4a/Arf expression is a biomarker of aging. J Clin Invest. 2004;114:1299–307.
15. Diekman BO, Sessions GA, Collins JA, et al. Expression of p16INK4a is a biomarker of chondrocyte aging but does not cause osteoarthritis. Aging Cell. 2018;17:e12771.
16. Faust HJ, Zhang H, Han J, et al. IL-17 and immunologically induced senescence regulate response to injury in osteoarthritis. J Clin Invest. 2020;130:5493.
17. Gale DR, Chaisson CE, Totterman SM, et al. Meniscal subluxation: association with osteoarthritis and joint space narrowing. Osteoarthritis Cartilage. 1999;7:526–32.
18. Lohmander LS, Englund PM, Dahl LL, et al. The long-term consequence of anterior cruciate ligament and meniscus injuries: osteoarthritis. Am J Sports Med. 2007;35:1756–69.
19. Song Y, Greve JM, Carter DR, et al. Meniscectomy alters the dynamic deformational behavior and cumulative strain of tibial articular cartilage in knee joints subjected to Cyclic loads. Osteoarthritis Cartilage. 2008;16:1545–54.
20. Englund M, Guermazi A, Lohmander LS. The meniscus in knee osteoarthritis. Rheum Dis Clin North Am. 2009;35:579–90.
21. Englund M. The role of the meniscus in osteoarthritis genesis. Med Clin North Am. 2009;93:37–43. x.
22. Tsujii A, Nakamura N, Horibe S. Age-related changes in the knee meniscus. Knee. 2017;24:1262–70.
23. Kwon H, Brown WE, Lee CA, et al. Surgical and tissue engineering strategies for articular cartilage and meniscus repair. Nat Rev Rheumatol. 2019;15:550–70.

24. Nebelung S, Tingart M, Pufe T, et al. Ex vivo quantitative multiparametric MRI mapping of human meniscus degeneration. Skeletal Radiol. 2016;45:1649–60.
25. Muhammad H, Schminke B, Bode C, et al. Human migratory meniscus progenitor cells are controlled via the TGF-β pathway. Stem Cell Rep. 2014;3:789–803.
26. Segawa Y, Muneta T, Makino H, et al. Mesenchymal stem cells derived from synovium, meniscus, anterior cruciate ligament, and articular chondrocytes share similar gene expression profiles. J Orthop Res Off Publ Orthop Res Soc. 2009;27:435–41.
27. Shen W, Chen J, Zhu T, et al. Osteoarthritis prevention through meniscal regeneration induced by intra-articular injection of meniscus stem cells. Stem Cells Dev. 2013;22:2071–82.
28. Sun H, Wen X, Li H, et al. Single-cell RNA-seq analysis identifies meniscus progenitors and reveals the progression of meniscus degeneration. Ann Rheum Dis. 2020;79:408–17.
29. Fu W, Chen S, Yang R, et al. Cellular features of localized microenvironments in human meniscal degeneration: a single-cell transcriptomic study. eLife. 2022;11:e79585.
30. Sun H, Zhang W, Liu F, et al. Single-cell RNA sequencing reveals the cell types heterogenicity of human discoid lateral meniscus cells. J Cell Physiol. 2022;237:2469–77.
31. Kim H-E, Shin Y, Jung IJ, et al. Overexpression of secretory leukocyte peptidase inhibitor (SLPI) does not modulate experimental osteoarthritis but May be a biomarker for the disease. Osteoarthritis Cartilage. 2021;29:558–67.
32. Choi W-S, Lee G, Song W-H, et al. The CH25H–CYP7B1–RORα axis of cholesterol metabolism regulates osteoarthritis. Nature. 2019;566:254–8.
33. Glasson SS, Chambers MG, Van Den Berg WB, et al. The OARSI histopathology initiative– recommendations for histological assessments of osteoarthritis in the mouse. Osteoarthritis Cartilage. 2010;18:S17–23.
34. Quinn R. Comparing Rat's to human's age: how old is my rat in people years? Nutr Burbank Los Angel Cty Calif. 2005;21:775–7.
35. Trapnell C, Cacchiarelli D, Grimsby J, et al. Pseudo-temporal ordering of individual cells reveals dynamics and regulators of cell fate decisions. Nat Biotechnol. 2014;32:381.
36. Gulati GS, Sikandar SS, Wesche DJ, et al. Single-cell transcriptional diversity is a hallmark of developmental potential. Science. 2020;367:405–11.
37. Draghici S, Khatri P, Tarca AL, et al. A systems biology approach for pathway level analysis. Genome Res. 2007;17:1537.
38. Saul D, Kosinsky RL, Atkinson EJ, et al. A new gene set identifies senescent cells and predicts senescence-associated pathways across tissues. Nat Commun. 2022;13:4827.
39. Barbie DA, Tamayo P, Boehm JS, et al. Systematic RNA interference reveals that oncogenic KRAS-driven cancers require TBK1. Nature. 2009;462:108–12.
40. Ke L, He Q, Qu J, et al. Bone-protective effects of neutralizing angiopoietin-like protein 4 monoclonal antibody in rheumatoid arthritis. Mol Ther J Am Soc Gene Ther. 2024;32:4497–513.
41. Benito MJ, Veale DJ, FitzGerald O, et al. Synovial tissue inflammation in early and late osteoarthritis. Ann Rheum Dis. 2005;64:1263–7.
42. Mathiessen A, Conaghan PG. Synovitis in osteoarthritis: current Understanding with therapeutic implications. Arthritis Res Ther. 2017;19:18.
43. Burr DB, Gallant MA. Bone remodelling in osteoarthritis. Nat Rev Rheumatol. 2012;8:665–73.
44. Lin P, Zhang G, Peng R, et al. Increased expression of bone/cartilage-associated genes and core transcription factors in keloids by RNA sequencing. Exp Dermatol. 2022;31:1586–96.
45. Heinonen J, Taipaleenmäki H, Roering P, et al. Snorc is a novel cartilage specific small membrane proteoglycan expressed in differentiating and articular chondrocytes. Osteoarthritis Cartilage. 2011;19:1026–35.
46. Buechler MB, Pradhan RN, Krishnamurty AT, et al. Cross-tissue organization of the fibroblast lineage. Nature. 2021;593:575–9.
47. Gao Y, Li J, Cheng W, et al. Cross-tissue human fibroblast atlas reveals myofibroblast subtypes with distinct roles in immune modulation. Cancer Cell. 2024;42:1764–e178310.
48. Iezaki T, Ozaki K, Fukasawa K, et al. ATF3 deficiency in chondrocytes alleviates osteoarthritis development. J Pathol. 2016;239:426–37.
49. James CG, Woods A, Underhill TM, et al. The transcription factor ATF3 is upregulated during chondrocyte differentiation and represses Cyclin D1 and A gene transcription. BMC Mol Biol. 2006;7:30.
50. Lin J, Ruan W, Zhang J, et al. Exploring the role of ATF3 and ferroptosis-related RNA expression in osteoarthritis: an RNA analysis approach to immune infiltration. Int J Biol Macromol. 2024;283:137872.
51. Tang Y, Zhuo D, Yu Y, et al. Single-cell RNA sequencing reveals the CRTAC1 + population actively contributes to the pathogenesis of spinal ligament degeneration by SPP1 + macrophage. Aging Cell. 2024;23:e14320.
52. Zhang J, Zhu J, Zhao B, et al. LTF induces senescence and degeneration in the meniscus via the NF-κB signaling pathway: A study based on integrated bioinformatics analysis and experimental validation. Front Mol Biosci. 2023;10:1134253.
53. Chen M, Zhou S, Shi H, et al. Identification and validation of pivotal genes related to age-related meniscus degeneration based on gene expression profiling analysis and in vivo and in vitro models detection. BMC Med Genomics. 2021;14:237.
54. Yang H, Chen C, Chen H, et al. Navitoclax (ABT263) reduces inflammation and promotes chondrogenic phenotype by clearing senescent Osteoarthritic chondrocytes in osteoarthritis. Aging. 2020;12:12750–70.
55. Aimono Y, Endo K, Sekiya I. Cellular senescence contributes to spontaneous repair of the rat meniscus. Aging Cell. 2025;24:e14385.
56. McQueen AE, Kanamaluru D, Yan K, et al. The C-terminal fibrinogen-like domain of angiopoietin-like 4 stimulates adipose tissue lipolysis and promotes energy expenditure. J Biol Chem. 2017;292:16122–34.
57. Cushing EM, Chi X, Sylvers KL, et al. Angiopoietin-like 4 directs uptake of dietary fat away from adipose during fasting. Mol Metab. 2017;6:809–18.
58. Zhu P, Goh YY, Chin HFA, et al. Angiopoietin-like 4: a decade of research. Biosci Rep. 2012;32:211–9.
59. Carbone C, Piro G, Merz V, et al. Angiopoietin-Like proteins in angiogenesis, inflammation and Cancer. Int J Mol Sci. 2018;19:431.
60. Knowles HJ. Multiple roles of Angiopoietin-Like 4 in osteolytic disease. Front Endocrinol. 2017;8:80.
61. Murata M, Yudo K, Nakamura H, et al. Hypoxia upregulates the expression of angiopoietin-like-4 in human articular chondrocytes: role of angiopoietin-like-4 in the expression of matrix metalloproteinases and cartilage degradation. J Orthop Res. 2009;27:50–7.
62. Hermann LM, Pinkerton M, Jennings K, et al. Angiopoietin-like-4 is a potential angiogenic mediator in arthritis. Clin Immunol. 2005;115:93–101.
63. Swales C, Athanasou NA, Knowles HJ. Angiopoietin-Like 4 is Over-Expressed in rheumatoid arthritis patients: association with pathological bone resorption. PLoS ONE. 2014;9:e109524.
64. Ke L, He Q, Qu J, et al. Bone-protective effects of neutralizing angiopoietin-like protein 4 monoclonal antibody in rheumatoid arthritis. Mol Ther. 2024;32:4497–513.
65. Wang W, Liu Y, Hao J, et al. Comparative analysis of gene expression profiles of hip articular cartilage between non-traumatic necrosis and osteoarthritis. Gene. 2016;591:43–7.
66. Rangkasenee N, Murani E, Schellander K, et al. Gene expression profiling of articular cartilage reveals functional pathways and networks of candidate genes for osteochondrosis in pigs. Physiol Genomics. 2013;45:856–65.
67. Snelling S, Rout R, Davidson R, et al. A gene expression study of normal and damaged cartilage in anteromedial gonarthrosis, a phenotype of osteoarthritis. Osteoarthritis Cartilage. 2014;22:334–43.
68. Jia C, Li X, Pan J et al. Silencing of Angiopoietin-Like protein 4 (Angptl4) decreases Inflammation, Extracellular matrix degradation, and Apoptosis in Osteoarthritis via the Sirtuin 1/NF-κB pathway. *Oxid Med Cell Longev*2022;2022: 1135827.
69. Li L, Chong HC, Ng SY, et al. Angiopoietin-like 4 increases pulmonary tissue leakiness and damage during influenza pneumonia. Cell Rep. 2015;10:654–63.
70. SkeletalAtlas. https://www.boneatlas.uma.es/easy_gdb/ (accessed 21March, 2025).
71. Wang X, Chang H-C, Gu X, et al. Renal lipid accumulation and aging linked to tubular cells injury via ANGPTL4. Mech Ageing Dev. 2024;219:111932.
72. Wen Y, Zhang X, Liu H, et al. SGLT2 inhibitor downregulates ANGPTL4 to mitigate pathological aging of cardiomyocytes induced by type 2 diabetes. Cardiovasc Diabetol. 2024;23:430.
73. Tsukasaki M, Takayanagi H. Osteoimmunology: evolving concepts in bone-immune interactions in health and disease. Nat Rev Immunol. 2019;19:626–42.

Publisher's note